JOURNAL OF CATALYSIS **101,** 227–237 (1986)

Adsorption and Reaction of Pyridine on Alkaline Earth Oxides as Studied by UV–Visible Diffuse Reflectance Spectroscopy

ADRIANO ZECCHINA* AND FRANK S. STONE†,[1]

**Istituto di Chimica Fisica, Università di Torino, Corso M. D'Azeglio 48, 10125 Torino, Italy; and †School of Chemistry, University of Bath, Bath BA2 7AY, England*

Received September 4, 1985; revised April 18, 1986

The adsorption of pyridine at room temperature on MgO, CaO, and SrO pre-outgassed at 1073 K gives rise to strong absorption bands in the near-UV and visible between 40,000 and 10,000 cm^{-1}. The development of these bands has been studied alongside the changes in the intrinsic UV spectra arising from excitation at low-coordinate surface O^{2-} ions (surface excitons). The exciton spectra are selectively eroded by the adsorption of pyridine.

The spectral changes at $\bar{\nu} < 40{,}000$ cm^{-1} are the sum of a reversible effect due to adsorption of pyridine as neutral molecules and an irreversible effect initiated by heterolytic dissociative chemisorption ($C_5H_5N \rightarrow C_5H_4N^- + H^+$) at the strongly basic oxide surface. The latter process is followed by coupling of $C_5H_4N^-$ anions to form bipyridyl anions and other carbanionic derivatives, characterised by absorption at ca. 25,000 and 20,000–15,000 cm^{-1}. The negatively charged organic species are formed from pyridine without the need for electron transfer from the oxide. The ease of formation of the anions increases on passing from MgO to CaO and SrO, in agreement with the increasing basicity of the oxides.

The effect of oxygen after exposure to pyridine is to destroy the absorption spectra due to the organic anions and to produce on all three oxides a new absorption band at 21,000 cm^{-1}. This band is ascribed to adsorbed O_2^-, formed by electron transfer from the pyridine-derived anions and located in their vicinity.

INTRODUCTION

The interaction of pyridine (Py) with outgassed alkaline earth oxides (*1–3*) leads to an intense coloration and to the production of an ESR spectrum. MgO, CaO, and SrO all show a similar behaviour. There is general agreement that the effects are due to the formation of negative ions and to a coupling reaction producing bipyridyl species. This conclusion is supported by separate studies which have been made on the direct adsorption of 2,2′-bipyridyl (*4*) and 4,4′-bipyridyl (*5*).

The ESR spectrum of adsorbed pyridine is poorly resolved and has attracted little attention. However, the coloured products resulting from pyridine adsorption are reactive towards oxygen (*1–3*), and among the side reactions is the formation of O_2^-. This aspect has been investigated rather fully (*6, 7*), since the O_2^- radical ion has a characteristic and well-resolved ESR spectrum which is amenable to detailed analysis.

The O_2^- ion has been a valuable prototype anion in the study of electron transfer processes on oxides in general (*8*). For transition metal oxides, one may be confident that the cation of the oxide is the source of the electron involved in the formation of adsorbed O_2^- from gaseous oxygen. For non-transition metal oxides, however, the situation is much less clear. It has been known for many years that O_2^- ions can be formed on MgO, but it must first be pre-irradiated (*9, 10*). Organic anions, however, e.g., those of trinitrobenzene and tetracyanoethylene, form on well-outgassed surfaces of MgO without pre-irradiation of the oxide (*11*). These and related studies led to the hypothesis (*12*) that negatively charged species form on basic oxides as a

---

[1] To whom correspondence should be addressed.

0021-9517/86 $3.00

result of direct electron transfer from O^{2-} ions in low coordination (LC) on the surface of the oxide. On this basis, pyridine could potentially form negative pyridine ions by direct electron transfer from O^{2-}_{LC} ions. An alternative hypothesis (*13*) is that negatively charged species form from organic molecules (XH) by heterolytic dissociation of a carbon–hydrogen bond

$$XH \rightleftharpoons X^- + H^+$$

at the basic oxide surface, the proton being held at the O^{2-}_{LC} ion. On the first hypothesis, the molecule is seen as probing the electron-donor properties of surface O^{2-}_{LC} ions, whilst on the second it is to be regarded as sensing the concerted action of $M^{2+}_{LC}O^{2-}_{LC}$ surface pairs in dissociating polarizable bonds by an acid–base interaction.

In the present study we concentrate on diffuse reflectance spectroscopy. For ionic oxides, reflectance spectroscopy in the UV–visible is a sensitive method for studying at one and the same time the properties of the adsorbed species and those of the adsorbing centres. Applied to pyridine adsorption on the alkaline earth oxides, it is likely to be the spectroscopic method of most value in discriminating between the electron-donor and acid–base hypotheses. Although the work already cited includes a few measurements of the electronic spectra of adsorbed pyridine on MgO (*1, 2*) and SrO (*3*), and the effect of oxygen, little attention has been paid to changes in the electronic spectrum of the solid. The reflectance spectra of well-outgassed polycrystalline MgO, CaO, and SrO (*14, 15*) show structured absorption lying on the low-energy side of the fundamental charge-transfer absorption. This absorption is excitonic in character and is due to transitions in the surface ions. Three well-defined bands (designated as exciton bands, I, II, and III) have been identified and analyzed (*16*) and their characteristics suggest that they are due to transitions of surface O^{2-} ions in 5-, 4- and 3-fold coordination (O^{2-}_{5C}, O^{2-}_{4C}, and O^{2-}_{3C}), respectively. In the present work we describe a detailed *comparative* investigation of the MgO–Py, CaO–Py, and SrO–Py systems, and we correlate the spectra of the adsorbate and adsorbent. We also report and discuss the spectral changes following the interaction of oxygen with chemisorbed pyridine.

EXPERIMENTAL

Pure polycrystalline MgO, CaO, and SrO, with BET surface areas of 240, 110, and 6 $m^2\ g^{-1}$, respectively, were prepared as previously described (*14, 15*).

Diffuse reflectance spectra were obtained with a Pye Unicam SP 700C spectrometer equipped with a reflectance attachment. The silica cell was of the same design as that described earlier (*14*), except that a side-arm was attached for outgassing the oxide away from contact with the optical window. This was particularly advantageous in the case of SrO for which the outgassing temperature (1273 K) was highest. MgO and CaO were outgassed at 1073 K. After this pretreatment the powdered oxide was transferred *in vacuo* to form a layer a few millimetres deep in contact with the optical window. All spectra were recorded at room temperature, and are presented as plots of reflectance (R'_∞) versus wavenumber. R'_∞ signifies that the reflectance refers to a sample deep enough to have the properties of an infinitely thick layer, and that the spectrum is compared against a standard (in the present case powdered silica of high optical purity).

Pyridine (BDH) was purified by the freeze–pump–thaw technique and was dosed as vapour in the pressure range up to 1.3 kPa (10 Torr). Oxygen was Specpure gas from BOC.

RESULTS

Magnesium Oxide

The reflectance spectrum of MgO outgassed at 1073 K and 10^{-4} Pa before pyridine adsorption is shown as the bold curve in Fig. 1. This reference spectrum for MgO

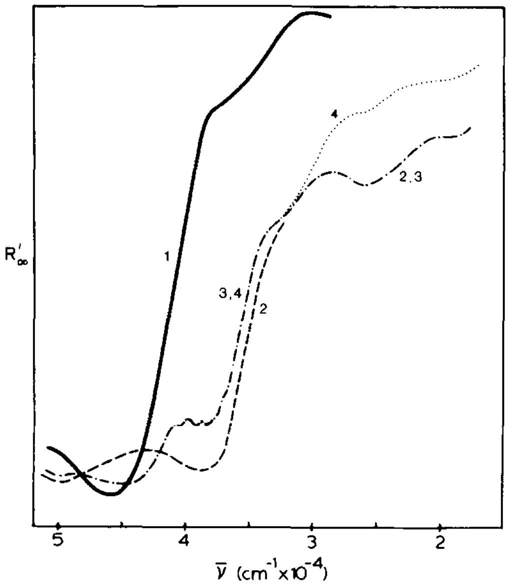

FIG. 1. UV-visible diffuse reflectance spectrum of pyridine adsorbed on MgO at room temperature. (1) Reference spectrum of pre-outgassed MgO (*14*), (2) in presence of pyridine at 260 Pa, (3) after evacuation, (4) after admission of oxygen at 1.6 kPa.

has actually been obtained in a small pressure of oxygen in order to quench the fluorescence (luminescence) (*17*) which otherwise causes an artefact in the reflectance spectrum *in vacuo* at high energy (*14*). The absorption band (reflectance minimum) at 46,000 cm^{-1} is due to surface exciton II and the shoulder at 35,000 cm^{-1} to surface exciton III (*14, 16*).

Admission of pyridine (Py) at 260 Pa (Fig. 1) destroys the band due to exciton II and develops new absorptions at ~50,000 (vs), 38,500 (vs), 32,500 (sh), 26,000 (w), 23,500 (sh), and 19,000 cm^{-1} (w). The effect of evacuation at room temperature (Fig. 1) is to decrease the intensity of the bands at 50,000 and 38,500 cm^{-1}, whilst the spectrum below 32,000 cm^{-1} is unaffected. The band centred at 38,500 cm^{-1} now shows fine structure, with five narrow components visible. A further effect of evacuation is partial restoration of exciton II absorption, but with lowered frequency (maximum shifted from 46,000 to 44,000 cm^{-1}).

Figure 1 also shows the effect of oxygen on preadsorbed pyridine. The absorptions at 26,000, 23,500, and 19,000 cm^{-1} are almost completely destroyed, and the shoulder at 32,000–33,000 is now clearly visible. No changes in the other regions of the spectrum are detected.

Calcium Oxide

The results with CaO are summarized in Fig. 2. The reference spectrum is that for CaO with fluorescence quenched in a low pressure of oxygen, as with MgO. It characterises the spectrum of the clean (reference) surface. The band at 35,500 cm^{-1} is the analogue of that at 46,600 cm^{-1} in MgO: this is surface exciton II, the exciton believed to be associated with 4-coordinate O^{2-} ions at steps and crystal edges (*16*). The broad band centred at 44,000 cm^{-1} is surface exciton I (*16*).

CaO outgassed at 1073 K was contacted with Py vapour at room temperature and the spectrum in 133 Pa of pyridine is shown in Fig. 2. Exciton II absorption at 35,500

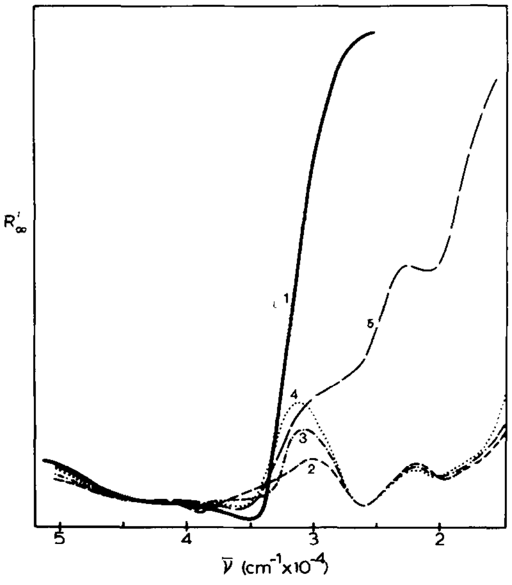

FIG. 2. Reflectance spectrum of pyridine adsorbed on CaO at room temperature. (1) reference spectrum of pre-outgassed CaO, (2) in presence of pyridine at 133 Pa, (3) after evacuation for 5 min, (4) after evacuation for 150 min, (5) after admission of oxygen at 250 Pa.

cm^{-1} is decreased, becomes more broad, and shifts to lower energies (31,000–35,000 cm^{-1}). New absorption appears as bands or shoulders at ~50,000 (s), 38,800 (s), 26,000 (vs), 20,000 (s), and ~17,000 cm^{-1} (m).

Evacuation at room temperature leads to gradual changes (in contrast to MgO where the change was fast) and two stages are illustrated in Fig. 2, namely, after pumping for 5 and 150 min, respectively. There is a decrease in the bands at 50,000 and 38,800 cm^{-1} and progressive restoration of exciton II to its original position, although not at its original intensity. The very strong band at 26,000 cm^{-1} is unaffected by desorption at room temperature, but there is erosion of the shoulder at 15,000–17,000 cm^{-1} and some upward shift of the 20,000 cm^{-1} band.

The effect of oxygen on preadsorbed pyridine is also shown in Fig. 2 for a pressure of 250 Pa. The bands at 26,000 and 20,000 cm^{-1} and the shoulder at 15,000–17,000 cm^{-1} are all destroyed. Absorption appears at ~30,000 and 21,000 cm^{-1}, which was either absent or obscured in the previous spectra. The band due to exciton II has increased in intensity as a result of the contact with oxygen.

Strontium Oxide

The band gap decreases in the sequence MgO, CaO, and SrO, so the spectrum of the solid extends to a lower wavenumber. With SrO it becomes possible to observe in the spectral range below 50,000 cm^{-1} both surface and bulk exciton absorption. The lower specific surface area of SrO means that the surface exciton spectrum is less intense than with MgO and CaO, with the result that the bulk and surface exciton absorptions are easily distinguished. Bulk excitons in SrO absorb at 44,000 cm^{-1} and above, whilst the surface excitons I and II exhibit their absorptions by reflectance minima at 37,000 and 32,000 cm^{-1}, respectively (*15, 16*). These features can be clearly seen in the reference spectrum for the outgassed surface shown as the bold curve in Fig. 3.

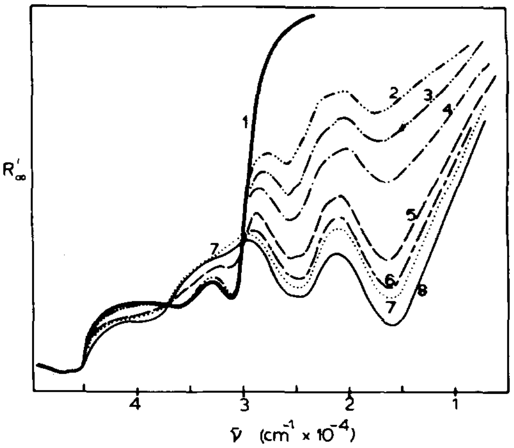

FIG. 3. Reflectance spectrum of pyridine adsorbed on SrO at room temperature. (1) reference spectrum of pre-outgassed SrO (with fluorescence quenched in a low pressure of oxygen), (2–8) successive admissions of doses of pyridine to give pressures of 13, 26, 40, 67, 80, 93, and 1300 Pa, respectively.

The effect of dosing pyridine is also illustrated in Fig. 3. Successive admissions of pyridine were made and the spectra at various residual pressures up to 1.3 kPa are shown. The absorptions due to surface excitons I and II are progressively reduced as the coverage of adsorbed species builds up. At the same time, new absorption develops at 37,000–44,000 cm^{-1}, with a band at ~39,000 cm^{-1} in the final spectrum. The most striking effect, however, is the progressive growth of two pronounced absorptions below 28,000 cm^{-1}, and the characteristics may be summarized as follows: (i) at low coverage there are bands with peaks (reflectance minima) at 25,700 and 17,500 cm^{-1} and shoulders at 24,000, 21,800, 15,500, and ~13,500 cm^{-1}; (ii) by high coverage the shoulder at 24,000 cm^{-1} has become a definite band with intensity even greater than that of the initial component at 25,700 cm^{-1} (due to the overlap the absorption maximum moves to lower $\bar{\nu}$ in the sequence of spectra); (iii) in a similar way the absorption peak at 17,500 cm^{-1} moves to lower $\bar{\nu}$ with increasing coverage, due in this case to the growth and ultimate domination of the absorption at 15,500 cm^{-1}; (iv) the absorption envelope of the 24,000–26,000 cm^{-1} bands grows less quickly with coverage than that of the bands at 15,500–17,500 cm^{-1}. These characteristics indicate that *several* adsorbed species are involved.

The effect of evacuating unadsorbed pyridine and subsequent outgassing at 373 K is shown in Fig. 4. There are three features to note. Firstly, the bands at 24,000 and 15,500 cm^{-1} are much decreased in intensity, whilst those at 25,700 and 17,500 cm^{-1} are not (a slight *increase* is detectable in these latter bands). These facts establish that at least two different species are involved (each one exhibiting two transitions), and that the one species can be transformed into the other by addition or removal of pyridine. Secondly, the band at 39,000 cm^{-1} disappears on pumping at room temperature. Finally, the absorption associated with surface excitons is partially restored, as manifested by the changes at 31,000–38,000 cm^{-1} as outgassing is continued.

The interaction of oxygen and pyridine on SrO is shown in Fig. 5. As with the MgO–Py–O_2 and CaO–Py–O_2 systems, the effect of oxygen is to destroy immediately all the coloured species associated with the bands at low $\bar{\nu}$. At the same time a new absorption peak (reflectance minimum) is manifested at 21,000 cm^{-1}, and a weak shoulder at about 27,000 cm^{-1} can also be discerned.

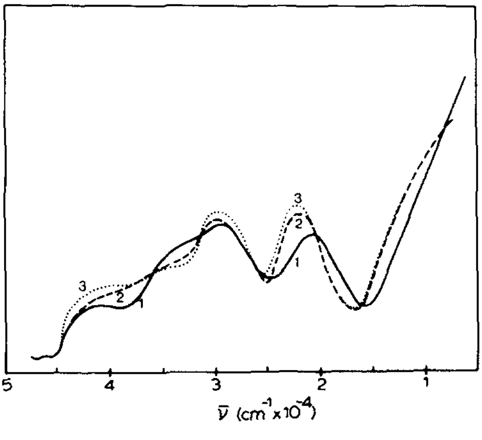

FIG. 4. Effect of evacuation on the reflectance spectrum of pyridine adsorbed on SrO. (1) in pyridine vapour at 1.3 kPa, (2) after evacuation for 10 h at room temperature, (3) after outgassing for 10 h at 373 K.

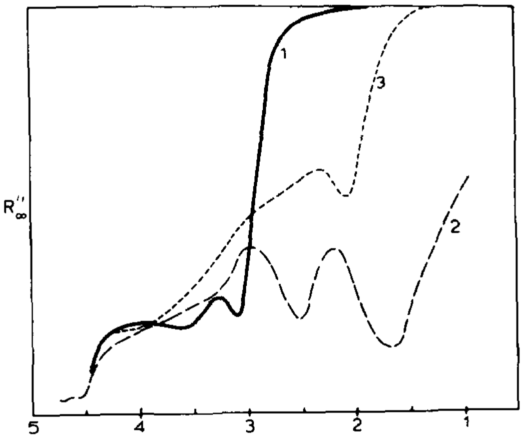

FIG. 5. Effect of oxygen on the reflectance spectrum of pyridine adsorbed on SrO. (1) reference spectrum, (2) in pyridine vapour at 1.3 kPa, (3) after evacuation and admission of O_2 at 133 Pa.

DISCUSSION

Spectrum of Adsorbed Pyridine

The admission of pyridine to the outgassed surfaces of MgO, CaO, and SrO gives rise in each case to an absorption band close to 39,000 cm^{-1}. With MgO, but not with CaO or SrO, it is possible to resolve several vibrational components when pyridine is at low coverage. This absorption band is readily identified as that of pyridine molecules, since pyridine in solution exhibits a similar band at 39,000 cm^{-1}, generally assigned as the lowest π–π^* transition (*18*). Free pyridine exhibits a second band at ~50,000 cm^{-1}, and this absorption is also evident in the pyridine spectra on MgO and CaO. These bands from adsorbed pyridine are pressure dependent and decrease upon evacuation. They are clearly due to weakly adsorbed Py, probably simply coordinated to surface cations (Lewis sites) through the lone pair on the nitrogen atom. This is supported by the following facts: (i) the resistance of the 39,000 cm^{-1} band to evacuation is in the order MgO > CaO $\geq$ SrO, as would be expected if the lone pair of Py is coordinated to Lewis centres of polarizing power decreasing with increasing cation radius, (ii) the vibrational fine structure is found only for Py on MgO, analogous to the observation (*18*) that in solution the fine structure is more easily observed in hydroxylic solvents where there is a strong interaction between the positive centers (the hydrogen atom) and the nitrogen lone pair.

The bands produced in the range 32,000–10,000 cm^{-1}, on the other hand, have no counterpart in the spectrum of free uncharged pyridine. Moreover, the bands remain after evacuation at room temperature. They must therefore be due to chemisorbed species derived from pyridine. The intensity of these bands (per unit of surface area) is in the order SrO > CaO $\gg$ MgO, which is the order of decreasing basicity, indicating that the species are produced by an acid–base (Py–O^{2-}) interaction. The low frequency is indicative of anions, and derivatives of pyridine with bands in the range observed are bipyridyl anions (*19*); such species could be produced by dimerization of dissociatively chemisorbed pyridine. We shall return to the spectra of these strongly adsorbed species after discussing the implications of the changes in the exciton spectra of the oxides due to exposure to pyridine.

Effect of Pyridine on the Surface Spectra of the Oxides

The bands associated with the surface states (the surface excitons I, II, and III, assigned to the low-coordinate O^{2-}_{5C}, O^{2-}_{4C}, and O^{2-}_{3C} ions, respectively) are affected by the adsorption of pyridine.

With MgO, the effect on exciton II is to shift the band (the prominent absorption at 46,000 cm^{-1}) to lower frequency. The effect is seen well in the low-coverage spectrum, where the displaced band is still distinguishable from the absorption band generated by the pyridine itself. The changes in this spectral region are reversible. This implies that the O^{2-}_{4C} ions (steps and edge sites) are not involved in the chemisorption which produces the irreversible changes in the spectrum below 30,000 cm^{-1}. Exciton I in MgO lies at too high an energy to be seen, so no comment can be made about the O^{2-}_{5C} ions. However, we would expect those ions to be less reactive than O^{2-}_{4C}. The O^{2-}_{3C} ions, on the other hand, are likely to be more reactive. Their absorption is the shoulder at 35,000 cm^{-1}. There are relatively few of these sites, and this is in accord with the relatively low intensity of the bands produced.

With CaO, Fig. 2 shows that exciton II (the strong absorption band at 35,500 cm^{-1}) undergoes two changes when pyridine is admitted. There is a shift of some absorption to lower frequency, and this a reversible effect, disappearing when pyridine is evacuated. However, there is also a concomitant irreversible effect, namely a genuine loss in intensity. The loss in intensity is accompanied by the production of a very intense spectrum below 30,000 cm^{-1}. The inference is that, unlike MgO where only O^{2-}_{3C} ions were active sites for promoting chemisorption to produce pyridine derivatives, a proportion of the O^{2-}_{4C} sites is now active. This is entirely compatible with the increased basicity of CaO, and the concept that basicity is influential in generating the species giving rise to absorption below 30,000 cm^{-1}.

Turning to SrO, the trend is seen to be continued. The irreversible effect is now the predominant one, eroding not only exciton II absorption but also in part that of exciton I, thereby establishing widespread participation of O^{2-}_{4C} ions and, in addition, involvement in this case of a proportion of the O^{2-}_{5C} ions, the ions on the {100} faces. Recalling the much lower specific surface area of the SrO sample (6 m^2 g^{-1}, compared with 110 m^2 g^{-1} for CaO and 240 m^2 g^{-1} for MgO), which is reflected in the less pronounced intensity of exciton I and II absorption, the spectrum developed below 30,000 cm^{-1} is pro rata extremely intense. The basicity criterion is further confirmed.

The above analysis shows that the overall effect of pyridine adsorption on the surface states is the sum of a *reversible effect*, dominant on MgO and associated with simple weak adsorption of the neutral pyridine molecule, and an *irreversible effect*, dominant on the much more basic SrO and associated with the formation of strongly chemisorbed anionic derivatives.

(a) The Reversible Effect. We now discuss the nature of the reversible effect. The "red shift" for exciton II in MgO and CaO is 2000 cm^{-1} or more. A similar effect is observed when NH_3 is adsorbed on the alkaline earth oxides (*20*) and also when certain adsorbates are weakly held on KI microcrystals (*21*). In the latter case, a systematic investigation of the effect on the surface excitonic transitions of I^- has established that there is a correlation between the downward shift in frequency produced by the adsorbate vapour (e.g. NH_3, CH_3CN, and $CH_3COC_2H_5$) and the shift produced in the absorption band of dissolved I^- ions when that same substance is used as a solvent. The inference is that the frequency of the excitations essentially localised on low-coordinate surface I^- ions is influenced by an environment of weakly adsorbed molecules in just the same way as those of dissolved I^- ions are by a cage of solvent molecules. This influence of solvents on the spectra of dissolved anions (especially I^-) is well documented (*22*), and is explained by the transition taking on the character of a partial charge transfer to the solvent (CTTS). The present results and the analogous studies of NH_3 adsorption (*20*) enable these ideas to be extended to low-coordinate O^{2-} ions on ionic oxide surfaces. The reversible effect is therefore ascribed to a "solvating" environment of weakly adsorbed Py molecules held on adjacent cations (and physically adsorbed Py on top). The excitation formerly localised on the exposed O^{2-}_{LC} ions becomes partially delocalised onto the adsorbate, giving the transition a partial charge-transfer-to-adsorbate (CTTA) character and shifting the absorption band to lower frequency.

(b) The Irreversible Effect. Chemisorption of pyridine producing strongly chemisorbed species simultaneously erodes the exciton spectrum of the surface oxide ions (O^{2-}_{LC}). This result is similar to that already reported (*14, 15*) for the chemisorption of H_2O and found also with alkenes (*13*). It is ascribed to the formation of surface OH^- ions as a result of dissociative chemisorption of pyridine ($C_5H_5N + O^{2-}_{LC} \rightarrow C_5H_4N^-_{ads} + OH^-$). The O^{2-}_{LC} surface states are destroyed in this process.

The Nature of the Strongly Adsorbed Organic Species

The absorption in the range 33,000–10,000 cm^{-1} observed after exposure of the oxides to pyridine and subsequent evacuation cannot be explained in terms of neutral Py or neutral Py derivatives such as donor-coordinated Py or bipyridyl. One has to invoke *negatively charged* species.

The simplest negative species is the Py^- radical, which could in principle form by simple electron transfer from O^{2-}_{LC} ions:

$$O^{2-}_{LC} + Py \rightarrow Py^- + O^-. \qquad (1)$$

There is some doubt about the spectrum of Py^-; Dodd *et al.* (*23*) suggest that bands at 42,500 and 30,000 cm^{-1} in solution spectra are typical for Py^- (with $\varepsilon_{42,500} > \varepsilon_{30,000}$), but later workers (*24*) attributed them to dimeric anions. However, the situation for the analogous anion of benzene (Bz^-) is better established: in this case there is less doubt that bands observed at 40,000 and 25,000 cm^{-1} (with $\varepsilon_{40,000} > \varepsilon_{25,000}$) are due to Bz^- (*25*). One may therefore infer that Py^- will not have transitions at frequencies lower than about 25,000 cm^{-1}. This is supported by the observation (*6*) that the radical anion of 4-picoline (where formation of dimeric species does not occur because the 4-position is blocked) has its lowest absorption at ~28,500 cm^{-1}. We conclude that the Py^- anion radical should show a pair of bands at 40,000–42,000 and 25,000–30,000 cm^{-1}, with the former more intense than the latter. For pyridine on our oxides, we observe a peak at ~25,000–26,000 cm^{-1} in all cases; however, the absence of a high intensity peak at 40,000–42,000 cm^{-1} suggests that Py^-, if present at all, is only contributing to a small extent to the 25,000–26,000 cm^{-1} absorption. Thus Reaction (1), if operating, cannot be the only process occurring at the surface. Other negatively charged species, formed by a different route, must be present. These considerations weigh heavily against the mechanism of simple electron transfer [Reaction (1)]. Moreover, at least in its simplest form, this mechanism is also unlikely since it leaves on the surface the species O^-, which due to its well-known reactivity (*27*) would not be expected to survive in the presence of pyridine.

The next most simple negative structure to consider is metallated pyridine, e.g., α-metallated Py on MgO, as would form by

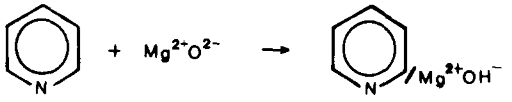

(2)

or, in shortened form, with XH written for pyridine Py,

$$XH + Mg^{2+}O^{2-} \rightarrow X^-|Mg^{2+}OH^-. \quad (2')$$

This reaction is the analogue of that known in homogeneous chemistry for metallating weakly acidic –CH with Li- or Mg-alkyls (*28*), as in

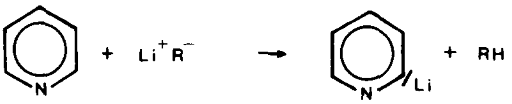

(3)

The ability of $Mg^{2+}_{LC}O^{2-}_{LC}$ surface ion pairs to react with R–H species to form R–Mg^{2+} and OH^- surface species has already been shown for acetylene (*29*), alkenes (*13*), NH_3 (*30*), and H_2 (*31*). As far as we are aware, the electronic spectrum of α-metallated Py is not known. However, one would expect it to be dominated by the n–π^* transition of the doublet at the metallated carbon, which is similar in nature to the n–π^* transition of the nonbonding doublet on the nitrogen in neutral pyridine. This latter occurs at ~35,000 cm^{-1} (*18*), so a band at similar $\bar{\nu}$ should be characteristic of metallated Py. This enables us to conclude that, if metallated Py is present, it is not responsible for the low-$\bar{\nu}$ bands observed in our spectra on all three oxides at 25,000–26,000 and 15,000–20,000 cm^{-1}. It could, however, possibly account for the shoulder at 32,000 cm^{-1} on MgO and the band at 32,000–34,000 cm^{-1} observed on SrO after exposure to Py and evacuation at room temperature.

To account for the low-$\bar{\nu}$ bands we must therefore invoke more complicated anionic species. We note evidence from the literature for two high intensity bands in the regions 25,000–26,000 and 16,000–20,000 cm^{-1} in the following species: (i) bipyridyl monoanions (*26*), (ii) bipyridyl dianions (*32*), (iii) negatively charged bipyridyl complexes of Ru (*19*), Cr, V, and Ti (*33*), (iv) the phenyl–pyridyl radical anion (*26*), (v) radical ions of biphenyl (*34*), (vi) terpyridyl monoanions (band at ~16,500 cm^{-1}) (*35*), and (vii) terphenyl monoanions (bands at 21,000–26,000 and 12,000 cm^{-1} (*36*). We may therefore confidently ascribe the strongly adsorbed coloured entities produced on MgO, CaO, and SrO to negatively charged polypyridyl species with general formula $(\text{pyridyl})_n^{z-}$, where $n = 2$ or 3 and $z = 1$ or 2.

Mechanism of Formation of Anionic Polypyridyl Species

The coupling of two or more pyridine rings to give anionic bipyridyl, terpyridyl, or higher species must necessarily be accompanied by hydrogen abstraction, and the mechanism for this will be analogous to that for Reaction (2). *The formation of these anions is convincing proof of the ability of the basic MgO, CaO, and SrO to abstract hydrogen by acid–base interaction.*

The first step is the heterolytic dissociation to give metallated pyridine [Reaction

(2) or (2′)]. This can then react by two distinct routes (I and II). In Route I a simple dimerization occurs, leading directly to the dinegative 4,4′-bipyridyl or 2,2′-bipyridyl ion:

$$2X^- \rightleftharpoons (X\text{–}X)^{2-} \quad (4)$$

In Route II the metallated Py reacts with excess pyridine (XH) by the processes

$$X^- + XH \rightleftharpoons (X\text{–}XH)^- \quad (5)$$

$$X^- + XH \rightleftharpoons XH^- + X\cdot \quad (6a)$$

$$X\cdot + X^- \rightleftharpoons (X\text{–}X)^- \quad (6b)$$

giving mononegative (radical) species on the surface.

Discrimination between Routes I and II in terms of the various mono- and dinegative species which can be formed is academic. For instance, in the same way that pyridine can abstract an electron from the metallated species [Reaction (6a)], it can abstract an electron from the dinegative species

$$(X\text{–}X)^{2-} + XH \rightleftharpoons (X\text{–}X)^- + XH^- \quad (7)$$

thereby giving the same products as from Route II.

The point which is important is that *negatively charged radical species can be produced without the need for electron transfer from the solid.* Their formation is simply a consequence of hydrogen abstraction as H^+ and electron transfer among adsorbed species, these processes being the true driving forces of the surface chemistry of pyridine on basic oxides.

The presence of a variety of radicals after chemisorption of pyridine is proved by the fact that a broad ESR signal is produced (*6, 7*). It is now clear, however, that these radical species represent only a fraction of the total products developed on the oxide surface: besides radicals there are also diamagnetic dianions and metallated species formed via a complex network of surface reactions. This situation is well in line with the kinetic behaviour of slow pyridine chemisorption and further reaction to coloured species described for MgO by Krylov *et al.* (*2*).

Coluccia *et al.* (*4, 5*) have demonstrated that coloured species are slowly generated if neutral bipyridyl is adsorbed directly from the gas phase on alkaline earth oxides. This again indicates formation of negative species, but it does not necessarily imply direct electron transfer from the solid. We believe that *also in this case* hydrogen abstraction leading to metallated bipyridyl species is the primary step of the chemisorption process, followed as before by electron transfer between co-adsorbed species. This accounts more satisfactorily for the fact that the process of generating the coloured species is slow.

Desorption Characteristics

As illustrated in detail for SrO in Fig. 4, the amount of adsorbed pyridine, both weakly and strongly adsorbed, can be reduced by pumping at ambient temperature or just above. Temperatures above 373 K must be avoided because cracking occurs. The question arises as to whether the sequence of reactions [Reactions (2), (4)–(7)] can be reversed by decreasing the pressure of pyridine.

From Fig. 4 it can be seen that the first important effect of pumping at room temperature is the loss of absorption at 38,000 cm^{-1}, which shows that neutral Py coordinated to Sr^{2+} cations is easily removed. The departure of this weakly adsorbed Py is accompanied by a shift to higher frequencies of the peaks due to the anionic species. This fact can be interpreted as follows. Anionic species tend to form "contact pairs" (*37*) with the surface Sr^{2+} cations. In the presence of co-adsorbed Py, the pairs are similar to the "solvent-separated pairs" of homogeneous solutions (*37*), while in the absence of Py the pairs become true "contact pairs," such as are observed in solvents with negligible solvating power. As contact pairs of carbanions have π–π^* bands at higher energy than the solvated pairs the shift to higher frequency when neutral Py is desorbed is explained.

The second important effect caused by

pumping at temperatures below 373 K is the growth of the peak at ~32,000 cm^{-1} which has been assigned to metallated pyridine. This means that some of the reactions (4)–(7) are reversible, at least partially. IR observations confirm this partial reversibility through an observed intensity decrease of surface anionic species bands on evacuation at beam temperature (*38*). Note that the reverse sequence of Reactions (5) and (6) does give XH (i.e., pyridine) in the gas phase and X^- (metallated pyridine) in the adsorbed state.

Effect of Oxygen on Anionic Pyridine-Derived Species

The effect of oxygen is to destroy virtually all the strongly adsorbed anionic species and metallated pyridine and to form a new band at 21,000 cm^{-1} (on SrO there is also some increase of absorption at ~39,000 cm^{-1}). The effect of O_2 on pyridine anion (Py^-) and various other anionic species derived from pyridine is well known in homogeneous solution chemistry, where electron transfer leading to O_2^- and neutral Py and derivatives occurs (*24*). One may expect that the same process will take place on the oxide surface, and this accounts for the production of the O_2^- ESR spectrum previously reported (*6, 7*). We may also recall the results of Coluccia *et al.* (*3*) which show the presence of luminescence from neutral 4,4′-bipyridyl following adsorption of pyridine on SrO and contact with oxygen. Bearing in mind the extensive literature on the oxygen sensitivity of metallated compounds in homogeneous organometallic chemistry (*39*), the results as a whole suggest the following reactions for the metallated pyridine formed by Reaction (2′), and its analogue on CaO and SrO, when exposed to oxygen at room temperature

$$X^- + O_2 \rightarrow X\cdot + O_2^- \qquad (8)$$

followed by

$$X\cdot + O_2 \rightarrow X\text{–}O\text{–}O\cdot \text{ (degradation products)} \qquad (9)$$

or

$$X\cdot + X\cdot \rightarrow X\text{–}X \qquad (10)$$

where X–X indicates adsorbed bipyridyl. Hence O_2^- is a main product of the interaction with oxygen. *This confirms the role of adsorbed anionic intermediates in surface processes leading to formation of* O_2^- (*13*).

As the spectra of anionic species are especially intense on CaO and SrO, indicative of high concentrations, a particularly high concentration of O_2^- can be expected on these oxides, and hence electronic transitions of adsorbed O_2^- may be observable. This species should have an electronic band in the visible or near-UV, and Kanzig and Cohen (*40*) have tentatively ascribed a band at 39,000 cm^{-1} in alkali halide crystals to O_2^-. More pertinently, a solution spectrum of O_2^- in pyridine has been reported by Slough (*41*) which shows bands at $\bar{\nu} >$ 30,000 cm^{-1} and at 22,000 cm^{-1}. The first band probably corresponds to that observed by Kanzig and Cohen (*40*) while the second is interpreted as a "charge-transfer-to-solvent" band where the O_2^- behaves as a donor and Py as an acceptor.

It is highly significant that this band at 22,000 cm^{-1} corresponds closely to the pronounced band observed on our oxides at 21,000 cm^{-1} after oxygen contact; moreover, the high frequency band occurs in the same region as that where an absorption clearly develops on SrO after O_2 treatment. Recalling that much of the SrO surface is populated by adsorbed pyridine and bipyridyl after exposure to O_2, we conclude that the band at 21,000 cm^{-1} is due to O_2^- "solvated" by an environment of adsorbed Py and bipyridyl.

The effect of Py and its derivatives on the spectrum of O_2^- (shift to lower $\bar{\nu}$ caused by the adsorption analogue of solvation) is similar to that reported for O_{4C}^{2-} transitions (exciton II) in an earlier section, and for the effect of NH_3 molecules on the spectrum of adsorbed NH_2^- on MgO (*20*).

ACKNOWLEDGMENTS

The authors are indebted to Professor E. Garrone for stimulating discussions on this work and they also express their thanks to Dr. M. A. Trevethan for obtaining the spectra on strontium oxide.

REFERENCES

1. Iizuka, T., and Tanabe, K., *Bull. Chem. Soc. Japan* **48,** 2527 (1975).
2. Krylov, O. V., Spiridonov, K. N., and Fokina, E. A., *Kinet. Catal. (Engl. Transl.)* **18,** 984 (1977).
3. Coluccia, S., Hemidy, J. F., and Tench, A. J., *J. Chem. Soc. Faraday Trans. 1* **74,** 2763 (1978).
4. Coluccia, S., Chiorino, A., Guglielminotti, E., and Morterra, C., *J. Chem. Soc. Faraday Trans. 1* **75,** 2188 (1979).
5. Coluccia, S., Garrone, E., and Morterra, C., *Z. Phys. Chem.* **124,** 201 (1981).
6. Che, M., Tench, A. J., Coluccia, S., and Zecchina, A., *J. Chem. Soc. Faraday Trans. 1* **72,** 1553 (1976).
7. Che, M., Coluccia, S., and Zecchina, A., *J. Chem. Soc. Faraday Trans. 1* **74,** 1324 (1978).
8. Che, M., and Tench, A. J., *Adv. Catal.* **32,** 1 (1983).
9. Lunsford, J. H., and Jayne, J. P., *J. Chem. Phys.* **44,** 1487 (1966).
10. Tench,. A. J., and Nelson, R. L., *J. Chem. Phys.* **44,** 1714 (1966).
11. Tench, A. J., and Nelson, R. L., *Trans. Faraday Soc.* **63,** 2254 (1967).
12. Cordischi, D., Indovina, V., and Cimino, A., *J. Chem. Soc. Faraday Trans. 1* **70,** 2189 (1974); Indovina, V., and Cordischi, D., *J. Chem. Soc. Faraday Trans 1* **78,** 1705 (1982).
13. Garrone, E., Zecchina, A., and Stone, F. S., *J. Catal.* **62,** 396 (1980).
14. Zecchina, A., Lofthouse, M. G., and Stone, F. S., *J. Chem. Soc. Faraday Trans. 1* **71,** 1476 (1975).
15. Zecchina, A., and Stone, F. S., *J. Chem. Soc. Faraday Trans. 1* **72,** 2346 (1976).
16. Garrone, E., Zecchina, A., and Stone, F. S., *Philos. Mag.* **42,** 683 (1980).
17. Tench, A. J., and Pott, G. T., *Chem. Phys. Lett.* **26,** 590 (1974); Shvets, V. A., Kuznetsov, A. V., Fenin, V. A., and Kazansky, V. B., *J. Chem. Soc. Faraday Trans. 1* **81,** 2913 (1985).
18. Halverson, F., and Hirt, R. C., *J. Chem. Phys.* **19,** 711 (1951).
19. Heath, G. A., Yellowlees, L. J., and Braterman, P. S., *J. Chem. Soc. Chem. Comm.*, 287 (1981).
20. Garrone, E., and Stone, F. S., *in* "Adsorption and Catalysis on Oxide Surfaces" (M. Che and G. C. Bond, Eds.), p. 97. Elsevier, Amsterdam, 1985.
21. Chiorino, A., Garrone, E., Ghiotti, G., and Zecchina, A., *J. Chem. Soc. Faraday Trans. 2* **78,** 857 (1982).
22. Blandamer, M. J., and Fox, M. F., *Chem. Rev.* **70,** 59 (1970).
23. Dodd, J. W., Hopton, F. J., and Hush, N. S., *Proc. Chem. Soc. London,* 61 (1962).
24. Chaudhuri, J., Kume, S., Jagur-Grodzinski, J., and Swarc, M., *J. Amer. Chem. Soc.* **90,** 6421 (1968).
25. Moore, J. C., Thornton, C., Coller, W. B., and Devlin, J. P., *J. Phys. Chem.* **85,** 350 (1981).
26. Kalyanaraman, V., Rao, C. N. R., and George, M. V., *J. Chem. Soc. B,* 2406 (1971).
27. Che, M., and Tench, A. J., *Adv. Catal.* **31,** 77 (1982).
28. Mallen, J. M., and Bebb, R. L., *Chem. Rev.* **69,** 693 (1969).
29. Stone, F. S., and Zecchina, A., *in* "Proceedings, International Congress on Catalysis, 6th (London, 1976)" (G. C. Bond, P. B. Wells, and F. C. Tompkins, Eds.) p. 162. The Chemical Society, London, 1977.
30. Garrone, E., and Stone, F. S., *in* "Proceedings, International Congress on Catalysis, 8th (Berlin, 1984)," Vol. III, p. 441. Verlag Chemie, Weinheim, 1984.
31. Coluccia, S., and Tench, A. J., *in* "Proceedings, International Congress on Catalysis, 7th (Tokyo, 1980)," p. 1154. Kodansha/Elsevier, Tokyo/Amsterdam, 1981.
32. Konig, E., and Kremer, S., *Chem. Phys. Lett.* **5,** 87 (1970).
33. Konig, E., and Herzog, S., *J. Inorg. Nucl. Chem.* **32,** 585, 601 (1970).
34. Hush, N. S., and Rowlands, J. R., *J. Chem. Phys.* **25,** 1076 (1956).
35. Kazuo, N., *Bull. Chem. Soc. Japan* **45,** 1943 (1972).
36. Shida, T., *J. Phys. Chem.* **82,** 991 (1978).
37. Hogan-Esch, T. E., *Adv. Phys. Org. Chem.* **15,** 153 (1977).
38. Zecchina, A., and Coluccia, S., to be published.
39. Sosnovsky, G., and Brown, J. H., *Chem. Rev.* **66,** 529 (1966).
40. Kanzig, W., and Cohen, M., *Phys. Rev. Lett.* **3,** 509 (1959).
41. Slough, W., *J. Chem. Soc. Chem. Commun.*, 184 (1965).